THE JOURNAL OF BIOLOGICAL CHEMISTRY VOL. 289, NO. 23, pp. 16239–16251, June 6, 2014

Regulation of TGF-β1-driven Differentiation of Human Lung Fibroblasts

EMERGING ROLES OF CATHEPSIN B AND CYSTATIN C[*]

Received for publication, December 11, 2013, and in revised form, April 22, 2014 Published, JBC Papers in Press, April 30, 2014, DOI 10.1074/jbc.M113.542407

Mariana Kasabova[‡1] **Alix Joulin-Giet**[‡], **Fabien Lecaille**[‡], **Brendan F. Gilmore**[§], **Sylvain Marchand-Adam**[‡], **Ahlame Saidi**[‡], **and Gilles Lalmanach**[‡2]

From the [‡]*INSERM U1100, Pathologies Pulmonaires: Protéolyse et Aérosolthérapie, Equipe 2: Mécanismes Protéolytiques dans l'Inflammation, Centre d'Etude des Pathologies Respiratoires, Université François Rabelais, Faculté de Médecine, F-37032 Tours, France and the* [§]*Queen's University Belfast, School of Pharmacy, McClay Research Centre, Belfast, BT9 7BL, United Kingdom*

Background: Proteolytic events are involved in the progression of lung fibrosis.
Results: Cathepsin B participates in lung fibroblast differentiation by triggering TGF-β1/Smad pathway. TGF-β1 up-regulates secretion of cystatin C.
Conclusion: TGF-β1 promotes cystatin C-dependent inhibition of extracellular matrix-degrading cathepsins.
Significance: Both cathepsin B and cystatin C could play a crucial role in fibrosis by favoring accumulation of ECM.

Lung matrix homeostasis partly depends on the fine regulation of proteolytic activities. We examined the expression of human cysteine cathepsins (Cats) and their relative contribution to TGF-β1-induced fibroblast differentiation into myofibroblasts. Assays were conducted using both primary fibroblasts obtained from patients with idiopathic pulmonary fibrosis and human lung CCD-19Lu fibroblasts. Pharmacological inhibition and genetic silencing of Cat B diminished α-smooth muscle actin expression, delayed fibroblast differentiation, and led to an accumulation of intracellular 50-kDa TGF-β1. Moreover, the addition of Cat B generated a 25-kDa mature form of TGF-β1 in Cat B siRNA-pretreated lysates. Inhibition of Cat B decreased Smad 2/3 phosphorylation but had no effect on p38 MAPK and JNK phosphorylation, indicating that Cat B mostly disturbs TGF-β1-driven canonical Smad signaling pathway. Although mRNA expression of cystatin C was stable, its secretion, which was inhibited by brefeldin A, increased during TGF-β1-induced differentiation of idiopathic pulmonary fibrosis and CCD-19Lu fibroblasts. In addition, cystatin C participated in the control of extracellular Cats, because its gene silencing restored their proteolytic activities. These data support the notion that Cat B participates in lung myofibrogenesis as suggested for stellate cells during liver fibrosis. Moreover, we propose that TGF-β1 promotes fibrosis by driving the effective cystatin C-dependent inhibition of extracellular matrix-degrading Cats.

Idiopathic pulmonary fibrosis (IPF)[3] is a chronic, irreversible lung disease of unknown etiology, leading to a progressive loss of lung function and ultimately death. IPF is the most common and severe form of idiopathic interstitial pneumonia with median survival of 3 years after diagnosis (1, 2). Despite multiple investigations (3), currently no effective treatments exist to hinder ongoing fibrosis. IPF is characterized by fibroblastic foci, which show increased activation response to pro-fibrogenic cytokines such as TGF-β1. Indeed, TGF-β1 plays a central role in fibrogenesis (4), and excessive expression of bioactive TGF-β1 was reported in lungs from IPF patients (5). TGF-β1 promotes the activation, proliferation, and differentiation of fibroblasts into α-smooth muscle actin (α-SMA)-expressing myofibroblasts that secrete excessive amounts of extracellular matrix (ECM) components. Accumulation and persistence of myofibroblasts is believed to contribute to the development of fibrosis (6). α-SMA expression, increased proliferative capacity, and enlarged generation and secretion of ECM proteins (collagen and fibronectin) are hallmarks of fibroblast differentiation in fibrotic disorders (7).

Fibrosis is also accompanied by abnormal proteolytic activities in lungs. Among various classes of proteases, there is now a growing body of evidence that cysteine cathepsins (Cats) participate in pulmonary homeostasis (8). Although their exact functions remain to be clarified, Cats are potent ECM-degrading enzymes (9, 10). They belong to the family C1 (11 cysteine cathepsins for the human genome: cathepsins B, H, L, S, C, K, O, F, V, X, and W; see MEROPS: the peptidase database: (11)) and have long been thought to be primarily involved in lysosomal end stage degradation of endocytosed proteins (12). They are

[*] This work was supported by la Région Centre (FibroCat Project 201000049823). We acknowledge the Institut National de la Santé et de la Recherche Médicale (INSERM) for institutional funding.
[1] Recipient of a doctoral fellowship from the Ministère de l'Education Nationale de la Recherche et de la Technologie, France.
[2] To whom correspondence should be addressed: INSERM, UMR 1100, Pathologies Pulmonaires: Protéolyse et Aérosolthérapie, CEPR, Université François Rabelais, Faculté de Médecine, 10 Blvd. Tonnellé, F-37032 Tours cedex, France. Tel.: 33-247366151; Fax: 33-247366046; E-mail: gilles.lalmanach@univ-tours.fr.

[3] The abbreviations used are: IPF, idiopathic pulmonary fibrosis; BALF, bronchoalveolar lavage fluid; BFA, brefeldin A; Cat, cysteine cathepsin; CA-074, *N*-(L-3-trans-propylcarbamoyloxirane-2-carbonyl)-L-isoleucyl-L-proline; CA-074Me, L-3-trans-(propylcarbamyloxirane-2-carbonyl)-L-isoleucyl-L-proline methyl ester; E-64, L-3-carboxy-trans-2,3-epoxy-propionyl-leucylamide-(4-guanido)-butane; E-64d, (2*S*,3*S*)-trans-epoxysuccinyl-L-leucylamido-3-methylbutane ethyl ester; ECM, extracellular matrix; -SMA, -smooth muscle actin; Z, benzyloxycarbonyl; AMC, 7-amino-4-methyl coumarin.

also secreted into the pericellular environment or associated with cell surfaces and found in nuclei (13). Cats contribute to specialized processes such as histone proteolysis during embryonic stem cell differentiation, processing of neuropeptides and thyroid hormones, bone remodeling and resorption, hair cycle control, and antigen presentation (for review, see Ref. 14). Cats are also involved in a wide range of disorders (*e.g.* atherosclerosis, adiposity, angiogenesis, and tumor invasion), making them striking targets for new anti-protease drugs (15, 16). Their proteolytic activity is specifically regulated by their natural inhibitors, members of the cystatin superfamily (stefins, cystatins, and kininogens) (17, 18), suggesting that an imbalance between Cats and cystatins could be crucial for the breakdown of ECM components. Genetic inhibition of Cat B in a murine BDL (bile duct ligation) model reduced hepatic inflammation, collagen deposition, and fibrogenesis (19). Expression of Cat B is enhanced during hepatic stellate cell activation and parallels the increase of TGF-β1 and α-SMA, supporting that Cat B may drive hepatic stellate cell transdifferentiation and hence participates in liver fibrogenesis (20). Alternatively, it has been suggested that the inhibition of Cat S may disturb TGF-β1 signaling and impair the differentiation of fibroblasts in a murine model of myocardial infarction (21).

Particularly, Cats production is increased in chronic lung disorders such as silicosis, asthma, and cystic fibrosis, which could aggravate the severity of inflammation by contributing to the remodeling of the basement membrane and ECM (22, 23). Nevertheless, some apparently contrasting results were reported. For example, in a murine model of bleomycin-induced lung injury, overexpression of Cat K has been detected (24). In contrast, Cat K deficiency exacerbated lung fibrosis, whereas increased levels of Cat K reduced excessive ECM deposition (25). Also Brömme and co-workers (26) observed that drug-induced overexpression of Cats K and L might be beneficial in the therapy of lung fibrosis. Moreover TGF-β1 down-regulates both Cat K expression in fibroblasts favoring silica-induced lung fibrosis (27) and Cat L expression in lung epithelial cells (28). However, whether human Cats may directly drive lung fibroblast differentiation or whether modulation of proteolytic activities by their natural inhibitors may affect their fibrogenic potential has not been specifically addressed to date.

The purpose of this study was to assess the potential contribution of human Cats to the pathophysiology of pulmonary fibrosis. To fulfill this objective, we developed an experimental model of differentiated fibroblasts (human lung CCD-19Lu cells) and also used primary fibroblasts (explant culture) obtained by biopsies from patients with IPF. Our data support the notion that Cat B participates in myodifferentiation of both IPF and CCD-19Lu fibroblasts and that TGF-β1-dependent secretion of cystatin C may finely tune promotion of fibrosis by inhibiting Cats that are potent ECM-degrading enzymes.

EXPERIMENTAL PROCEDURES

Enzymes, Substrates, and Inhibitors—Human cathepsins B and L were supplied by Calbiochem (VWR International, Pessac, France). Papain was purchased from Boehringer (Roche Molecular Biochemicals). Human recombinant His-tagged cystatin C, human recombinant cystatin (stefin) B, and benzyloxycarbonyl-Phe-Arg-7-amino-4-methyl coumarin (Z-Phe-Arg-AMC) were obtained from R&D Systems (Minneapolis, MN). Biotinyl-$(PEG)_2$-LVG-DMK, a cystatin-like irreversible probe, was synthesized according to a previous procedure (29) except that a hydrophilic biotinylated linker (*N*-biotinyl-NH-$(PEG)_2$-COOH; Novabiochem; Merck) was added. The final product was analyzed by mass spectrometry: theoretical molecular weight, 854.07; experimental mass, m/z = 853.47. *N*-(4-Biphenylacetyl)-*S*-methylcysteine-D-Arg-Phe-β-phenethylamide was from Calbiochem. L-3-Carboxy-trans-2,3-epoxy-propionyl-leucylamide-(4-guanido)-butane (E-64), (2*S*,3*S*)-trans-epoxysuccinyl-L-leucylamido-3-methylbutane ethyl ester (E-64d), *N*-(L-3-trans-propylcarbamoyloxirane-2-carbonyl)-L-isoleucyl-L-proline (CA-074), L-3-trans-(propylcarbamyloxirane-2-carbonyl)-L-isoleucyl-L-proline methyl ester (CA-074Me), pepstatin A, EDTA, 4-(2-aminoethyl) benzenesulfonyl fluoride hydrochloride (Pefabloc), *S*-methyl thiomethanesulfonate, DTT, actinomycin D, and brefeldin A (BFA) were from Sigma-Aldrich.

Cell Culture—Human primary fibroblasts were cultured from IPF lung explants according to Akamine *et al.* (30). A written informed consent was obtained for the study (Biocollection DC 2010–1216, The University Hospital, CHU Bretonneau, Tours, France). The CCD-19Lu normal human lung cell line was purchased from the American Type Culture Collection (Manassas, VA). Both IPF and CCD-19Lu fibroblasts were cultured in completed Eagle's minimum essential medium supplemented with heat-inactivated fetal calf serum (20% for IPF cells and 10% for CCD-19Lu) and 1% penicillin/streptomycin (LGC Standards SARL, Molsheim, France) at 37 °C, in an atmosphere containing 5% CO_2. Cells were cultured up to passage 5.

TGF-β1 Treatment—The effect of TGF-β1 stimulation was determined by the addition of recombinant TGF-β1 (R&D Systems) to 80% confluent fibroblasts. TGF-β1 (0–10 ng/ml) was prepared in serum-free culture medium, and all experiments were performed under serum-free conditions. The cells were seeded into 6-well plates, cultured for 24 h, and then were treated with recombinant TGF-β1 at different time intervals after a 24-h starvation period. Untreated controls cells were similarly incubated in the absence of TGF-β1.

Pharmacological Inhibitors—CCD-19Lu cells were seeded into 6-well plates, cultured for 24 h, and serum-deprived for additional 24 h. Subsequently, both pharmacological inhibitors CA-074Me (10 μM) and E-64d (50 μM), respectively, were added 6 h before TGF-β1 treatment (10 ng/ml) in basal medium for 8 days. Control experiments were performed in the presence of CA-074Me and E-64d, respectively, in the absence of TGF-β1. For transcription inhibition studies, cells were pretreated with 10 μg/ml of actinomycin D 6 h before the addition of TGF-β1 (10 ng/ml) for 2 and 3 days, respectively. BFA experiments were performed by incubating fibroblasts with 0.5 μg/ml of BFA 2 h prior to addition of TGF-β1 (10 ng/ml) in basal medium for 2 days.

siRNAs, RT-PCR, and Real Time PCR—Specific predesigned siRNAs used to silence Cats B, K, and L and cystatin C expression and scrambled siRNA used as control came from Qiagen (Table 1). Fibroblasts were transfected with 40 nM siRNA in basal medium using HiPerFect transfection reagent (Qiagen). The mixture was transferred to a 6-well plate for 24 h. There-

TABLE 1
Small interfering RNA sequences and primers used for quantitative PCR experiments

Protein	Strand (5′ → 3′)	Sequences of siRNA	Sequences of PCR primers
Cat B	Sense	GCAUGAUUCUUUAAUAGAATT	AGAGTTATGTTTACCGAGGACCT
	Antisense	UUCUAUUAAAGAAUCAUGCTG	GCAGATCCGGTCAGAGATGG
Cat K	Sense	GCAGUAAUGACACCCUUUATT	CCTTGAGGCTTCTCTTGGTG
	Antisense	UAAAGGGUGUCAUUACUGCGG	GGGCTCTACCTTCCCATTCT
Cat L	Sense	GAUCCGAGUGUGAUUUGAATT	GGAAAACTGGGAGGCTTATCTC
	Antisense	UUCAAUCACACUCGGAUCTT	AGCATAATCCATTAGGCCACCA
Cystatin C	Sense	CCACGUGUACCAAGACCCATT	GATCGTAGCTGGGGTGAACT
	Antisense	UGGGUCUUGGUACACGUGGTT	CCTTTTCAGATGTGGCTGGT
Scrambled siRNA	Sense	UUCUCCGAACGUGUCACGU	
	Antisense	ACGUGACACGUUCGGAGAA	
α-SMA	Sense		CAGGGCTGTTTTCCCATCCAT
	Antisense		GCCATGTTCTATCGGGTACTTC
RNA 16S	Sense		ACGTGGCCCAGATTTATGCTAT
	Antisense		TGGAAGCCTCATCCACATATTTC

after cells were stimulated with recombinant TGF-β1 (10 ng/ml) for an additional 48 h. Total RNA was purified using the RNeasy Mini kit (Qiagen) according to the manufacturer's instructions. Total RNA (0.5 μg) was reverse transcribed using the RevertAid Moloney murine leukemia virus reverse transcriptase (Fermentas, Thermo Fisher Scientific, Villebon sur Yvette, France). Quantitative analysis of α-SMA and Cat mRNAs was performed with the MyiQ system (Bio-Rad) (reaction volume, 20 μl) using the Absolute SYBR Green fluorescent mix (Dominique Dutscher, Brumath, France). Sense and antisense primers for cathepsins, cystatin C, and α-SMA are reported in Table 1. For quantification of relative expression levels, the ΔΔCt method was used (normalization gene, human ribosomal protein S16 (RPS16).

Phosphorylation Analysis—CCD-19Lu cells were seeded into 6-well plates. At 24 h post-transfection, recombinant TGF-β1 (10 ng/ml) was added for 1 h according to (31). Activation of signaling pathways (*e.g.* Smad 2, Smad 3, p38 MAPK, and SAPK/JNK) was further analyzed by immunoblotting (see next paragraph). Cell layers were lysed in PhosphoSafe extraction reagent (Novagen-EMD Biosciences, Darmstadt, Germany), sonicated 15 s, and centrifuged at 4 °C for 10 min at 16,000 × *g*. Untreated controls cells were similarly incubated in the absence of TGF-β1.

Western Blot Analysis—Antibody dilution and source were as follows: mouse anti-α-smooth muscle actin (α-SMA) (1:1000) and mouse anti-β-actin (1:2000) were supplied by Sigma-Aldrich. Rabbit anti-human cathepsin B (1:1000) was from Calbiochem, and rabbit anti-human cathepsin K (1:1000) was from Fitzgerald (Interchim, Montluçon, France). Goat anti-human cathepsins L and S (1:1000), mouse anti-human cystatin C (1:500), and goat anti-human cystatin (stefin) B (1:1000) were from R&D Systems. Mouse anti-human TGF-β1 (1:1000) was purchased from Abcam (Cambridge, UK). Rabbit anti-human phospho-Smad 2, phospho-Smad 3, Smad-2, Smad-3, phospho-p38 MAPK, p38 MAPK, phospho-SAPK/JNK, and SAPK/JNK (1:1000) came from Cell Signaling Technology (Beverly, MA). Rabbit anti-human Smad-2 and Smad-3 (nonphosphorylated forms) and both anti-phospho-SAPK/JNK and SAPK/JNK antibodies were a kind gift from Dr. Emmanuelle Liaudet-Coopman (Institut de Recherche en Cancérologie de Montpellier (IRCM), Inserm U896, Université Montpellier 1, Montpellier, France). Goat anti-rabbit IgG-peroxidase conjugate, goat anti-mouse IgG-peroxidase conjugate, and rabbit anti-goat IgG-peroxidase conjugate were from Sigma-Aldrich.

At each time point, culture media were harvested in the conservative buffer A: 0.1 M sodium acetate buffer, pH 5.5, containing protease inhibitors (0.5 mM Pefabloc, 0.5 mM EDTA, 1 mM *S*-methyl thiomethanesulfonate, 0.04 mM pepstatin A). The culture medium was centrifuged for 5 min at 9000 × *g* at 4 °C to remove cell debris. Cell layers were washed once in ice-cold PBS and harvested by scraping in ice-cold buffer A. Extraction of proteins was performed by three freeze-thaw cycles using liquid nitrogen. The disrupted homogenate was then centrifuged (10 min at 9000 × *g* at 4 °C). The remaining membrane pellets were resuspended in buffer A and stored at −80 °C. Culture media were concentrated 50-fold. Protein concentration was determined by Bradford assay (Bio-Rad). Samples (cell layer extracts and culture media) were prepared in Laemmli buffer and boiled for 3 min. Concentrated culture media (60 μg/well) and cell layer lysates (10 μg/well) were loaded onto 12% SDS-PAGE, and electrophoresis was carried out under reducing conditions. Prestained molecular masses (Precision Plus Protein Standards) came from Bio-Rad. The separated proteins were transferred to a nitrocellulose membrane (Amersham Biosciences). The membranes were blocked with 5% nonfat powdered milk in PBS, 0.1% Tween 20 (PBS-T). Alternatively membranes were incubated with 5% BSA in Tris-buffered saline, 0.1% Tween 20 (TBS-T) for 1 h for anti-TGF-β1, phospho-Smad 2, phospho-Smad 3, Smad-2, Smad-3, phospho-p38 MAPK, p38 MAPK, phospho-SAPK/JNK, and SAPK/JNK antibodies. Following incubation with the primary antibodies (overnight at 4 °C under agitation), the secondary antibodies (1:5000) were added for 1 h at room temperature. Proteins were visualized by chemiluminescence (ECL Plus Western blotting detection system; Amersham Biosciences) according to the manufacturer's instructions. Constant loading in proteins was checked by incubation with a monoclonal anti-β-actin antibody. Bands were quantified by densitometric analysis using the ImageJ software (National Institutes of Health, Bethesda, MD).

Maturation of Intracellular TGF-β1 by Cat B—CCD-19Lu fibroblasts (2×10^5 cells) were seeded into 6-well plates and transfected with 40 nM of siRNA directed against Cat B in basal medium using HiPerFect transfection reagent (Qiagen). A scrambled siRNA (40 nM) and CA-074Me (10 μM) were used as

control. Twenty-four hours later, the medium was removed. Fibroblast differentiation was initiated by the addition of exogenous TGF-β1 (10 ng/ml) for an additional 48 h. Cell layers were harvested, and then lysates (10 μg of protein) were separated by 12% SDS-PAGE. Finally, after immunoblotting using a monoclonal anti-TGF-β1 antibody, variation of the expression level of intracellular pro-TGF-β1 (50-kDa form) was monitored. β-Actin was used as loading control.

Alternatively, Cat B siRNA-pretreated CCD-19Lu lysates (10 μg of protein) were incubated with exogenous Cat B (1 μM) at 30 °C for 3 h. Samples were then separated by 12% SDS-PAGE under reducing conditions, and the separated products were transferred to nitrocellulose membranes and immunoblotted. Control experiments were performed by preincubating cell lysates with CA-074 (10 μM) for 30 min.

Deglycosylation of Intracellular TGF-β1—CCD-19Lu lysates (10 μg/assay) were treated with endo-β-*N*-acetylglucosaminidase F1 (endoglycosidase F1) according to supplier recommendations (Calbiochem). Overnight incubation was performed at 30 °C in 50 mM sodium acetate buffer, pH 5.0, 25 mM EDTA, 0.5% Triton X-100, 1% 2-mercaptoethanol. Samples were further submitted to a 12% SDS-PAGE before Western blotting (anti-human TGF-β1).

Immunofluorescence—Cell layers grown onto 8-well Lab-Tek chamber slides were fixed in 4% paraformaldehyde and permeabilized with 0.3% Triton X-100 in PBS. Saturation was performed with 5% BSA in PBS for 1 h at room temperature. Samples were then incubated with a mouse anti-α-SMA antibody (Sigma-Aldrich) (1:100) for 2 h at room temperature, before the addition in darkness of an anti-mouse secondary antibody conjugated to Alexa Fluor 488 (Molecular Probes, Invitrogen) diluted 1:300 in blocking buffer (1 h). The nuclei were stained with Hoechst dye (1:300). Photomicrographs were acquired with a Leica DMR fluorescence microscope (Leica Microsystems GmbH, Wetzlar, Germany).

Measurement of Cysteine Cathepsin Activity and Cathepsin Inhibitory Potential—Peptidase activity was measured using Z-Phe-Arg-AMC as substrate. Assay buffer was 0.1 M sodium acetate buffer, pH 5.5, 5 mM DTT, 2 mM EDTA, and 0.01% Brij35 (polyethylene glycol lauryl ether; Pierce). The fluorimetric assay (λexc, 350 nm; λem, 460 nm) was performed in 96-well plates (Nunc A/S, Roskilde, Denmark) with a Gemini spectrofluorimeter (Molecular Devices). Alternatively cathepsin inhibitory potential was determined as previously detailed (32), except that increasing volumes (0–60 μl) of culture media were incubated with E-64 titrated papain (5 nM) in the assay buffer at 30 °C for 60 min. The residual papain activity was measured by monitoring the hydrolysis of Z-Phe-Arg-AMC (5 μM), and the inhibitory capacity was deduced (33).

Labeling of Active Cysteine Cathepsins by a Cystatin-derived Activity-based Probe—Culture media of CCD-19Lu cells were incubated for 1 h with Biotinyl-$(PEG)_2$-LVG-DMK (10 μM), an irreversible diazomethylketone, where the tripeptidyl moiety (*i.e.* LVG) corresponds to the N-terminal substrate-like segment of human cystatin C, in the assay buffer (see the former paragraph) at 30 °C according to Ref. 34. Samples were subjected to electrophoresis on 12% SDS-PAGE under reducing conditions. Subsequently, the proteins were electrotransferred to a nitrocellulose membrane, blocked with 3% BSA in PBS-T, and incubated with an extravidin-peroxydase conjugate (1:2500; Sigma Aldrich) 2 h at room temperature. Proteins were visualized by chemiluminescence (ECL Plus Western blotting detection system).

Collagen and Cystatin C Assays—Collagen content was determined by Sircol assay (Biocolor Ltd., Belfast, UK). Sirius red dye (1 ml) was added to culture media (100 μl) and mixed for 30 min. The collagen-dye complex was precipitated by centrifugation at 10,000 $\times$ *g* for 10 min and dissolved in 0.5 M NaOH. Absorbance was determined by spectrophotometry at 540 nm. The concentration of secreted human cystatin C was determined using a commercial DuoSet ELISA kit (R&D Systems). Briefly, mouse anti-human cystatin C was first incubated in 96-well plates overnight at room temperature. Cystatin C standards or culture media were then applied and incubated for 2 h at room temperature. After a washing step, biotinylated mouse anti-human cystatin C antibody was incubated for 2 h followed by streptavidin horseradish-peroxidase conjugate for 20 min. After washing, samples were incubated with 0.04% (v/v) H_2O_2 and orthophenylene diamine (0.4 mg/ml) in substrate buffer (50 mM phosphate buffer, 20 mM citric acid, pH 5.5) in the dark before adding H_2SO_4 (3 M) to stop the reaction. Absorbance was measured at 492 nm in a plate reader (VersaMax; Molecular Devices), and the concentration of cystatin C was deduced.

Statistical Analysis—All of the data were expressed as median values. Differences between IPF and control samples were determined using the nonparametric two-way Mann-Whitney U test. We used the Kruskal and Wallis nonparametric test to compare the effects of various chemicals and reagents on baseline conditions. The values represent means ± S.E. (*, $p < 0.1$; **, $p < 0.05$; ***, $p < 0.001$).

RESULTS

Characterization of Cysteine Cathepsins Expressed by IPF Fibroblasts—According to murine models of bleomycin-induced lung fibrosis (25, 26, 35) and liver fibrosis (20, 36), several lines of evidence support that cysteine cathepsins may be involved in TGF-β1-dependent myofibrogenesis and/or subsequent modulation of ECM (*e.g.* collagen and fibronectin) deposition. These statements prompted us to investigate whether human Cats participate in lung fibroblast differentiation. First, we characterized Cats expressed by human fibroblasts from IPF patients. Immunoreactive mature Cat L and Cat B (both double-chain and single-chain forms) and partly processed Cat K were detected in lysates of cell layers from IPF primary fibroblasts (Fig. 1*a*). Conversely, we did not detect Cat S (proform and mature enzyme) as reported for cardiac fibroblasts (21). Secreted Cats B, L, and K, but not Cat S, were mostly found as zymogens in culture media, whereas their mature forms were weakly stained (Fig. 1*b*). The protein expression outline of the secreted enzymes partly differed from those of bronchoalveolar lavage fluids (BALFs) from patients suffering from sarcoidosis or alveolar proteinosis (32), where mature Cat L was detected, as well from silicosis patients where Cats B and L were mainly observed as processed active forms (37). It also differs from those of sputum of cystic fibrosis patients, in which mature

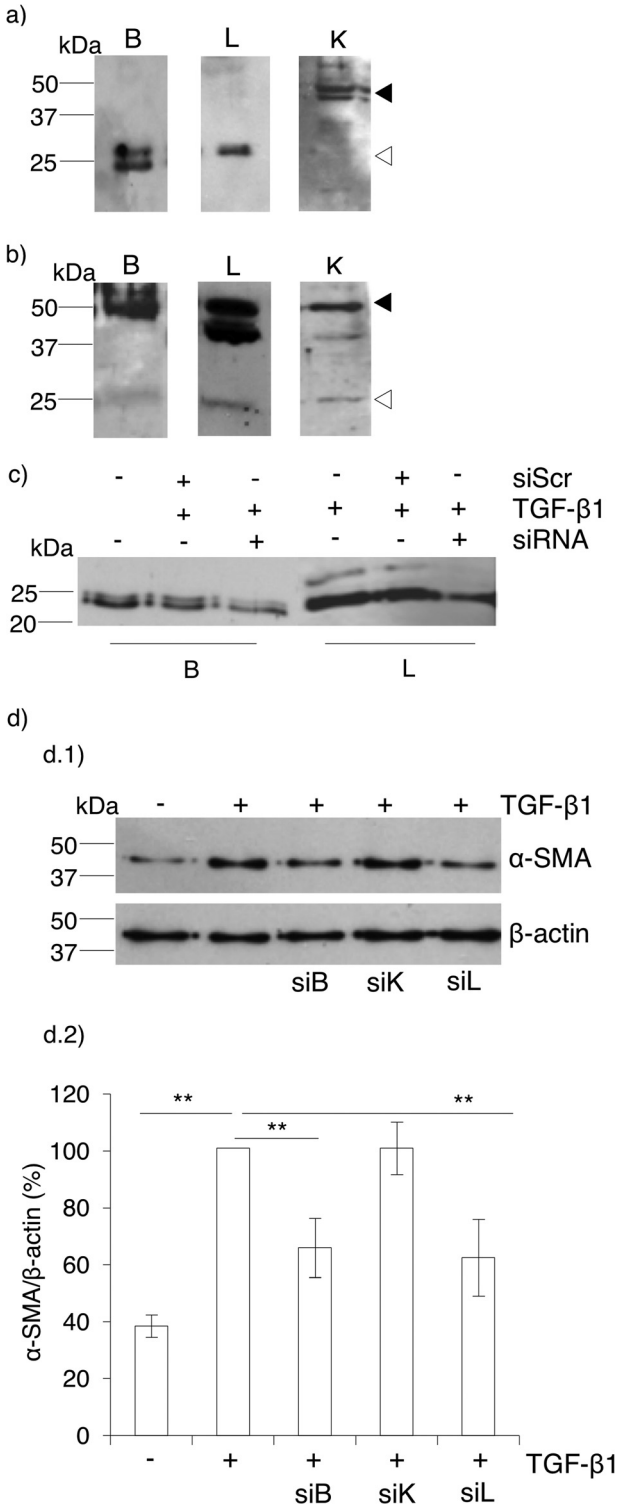

FIGURE 1. **Expression of cysteine cathepsins in human primary fibroblasts from IPF lung explants.** *a*, lysates (10 μg of proteins/well) were separated by SDS-PAGE (12%) under reducing conditions, transferred to nitrocellulose membrane, and analyzed with polyclonal antibodies against human Cats B, L, and K. *b*, culture media were concentrated 50-fold and samples (60 μg of proteins/well) were analyzed as described above. *Black arrows* correspond to Cat proforms, and *white arrows* correspond to mature enzymes. *c*, Western blot analysis of Cat B and Cat L after transfection by RNA interference (representative samples). *siScr*, scrambled siRNA; *siRNA*, siRNA directed against Cat B or Cat L. *d*, consequence of specific inhibition of Cat gene expression by siRNA on myofibrogenesis. Primary fibroblasts were transfected with siRNA directed against Cat B (*siB*), Cat K (*siK*), and Cat L (*siL*) 24 h prior to TGF-β1 (10 ng/ml) treatment for 2 days. *Panel 1*, immunodetection of α-SMA expression after Cat gene silencing using a monoclonal antibody directed against human α-SMA. A representative sample of three independent experiments is shown. *Panel 2*, densitometric analysis. The data were normalized to β-actin loading control ($n = 3$; **, $p < 0.05$).

secreted Cat B (mainly as its double-chain form) was intensely revealed (38) as has been shown in emphysema BALFs (39).

Silencing of Cats B and L by RNA Interference Impaired α-SMA Expression of IPF Fibroblasts—Transient knockdown of Cats B, K, and L was achieved by transfection of fibroblasts by specific small interfering RNAs. Inhibition of transcription was optimal at 72 h for Cat B (90% $\pm$ 3%, $n = 4$), Cat L (83% $\pm$ 4%, $n = 4$), and Cat K (85% $\pm$ 2%, $n = 3$), respectively, as determined by quantitative real time PCR. This message knockdown was confirmed by reduced protein levels of mature enzymes as observed by immunoblot analysis of lysates of cell layers (day 3) (Fig. 1*c*). Genetic silencing of Cats B and L but not Cat K reduced α-SMA expression (Fig. 1*d*, *panel 1*). Densitometric analysis confirmed that silencing of Cats B or L induced a significant ~1.5-fold reduction of α-SMA expression ($p < 0.05$), which support that both proteases may be involved in TGF-β1-driven fibroblast differentiation (Fig. 1*d*, *panel 2*). Nevertheless, double silencing of Cats B and L led to high cell mortality (approximately 66%) and did not allow us to assess whether the two siRNAs had an additive effect.

Characterization of Cats Expressed by Human Adult Lung CCD-19Lu Fibroblasts—Given the scarcity of clinical specimens (*e.g.* lung IPF biopsies), we decided to set up a cellular model for studying TGF-β1-driven differentiation of adult lung fibroblasts. As a prerequisite, we performed the detailed characterization of TGF-β1-driven differentiation of CCD-19Lu fibroblasts using α-SMA as marker (*i.e.* TGF-β1-inducible and dose-dependent transcription of α-SMA mRNA; concentration- and time-dependent induction of α-SMA protein translation as demonstrated by Western blot and immunofluorescence staining; Fig. 2*a*, *panels 1–4*), whereas increases in soluble collagen were determined by Sircol assay (Fig. 2*a*, *panel 5*). Quantitative analysis of mRNA expressions of Cats B, K, and L was done by PCR after reverse transcription of total RNA isolated from cell lysates. Messenger RNA levels of Cats B, K, and L remained stable in the presence of TGF-β1 (10 ng/ml) (data not shown). The mRNA level also remained unchanged following a pretreatment with actinomycin D, supporting that Cats are not transcriptionally regulated during TGF-β1-dependent differentiation (data not shown). A time-dependent increase of intracellular immunoreactive Cat L was observed during differentiation (Fig. 2*b*, *panels 1* and *2*), whereas a faint level of intracellular pro-Cat K was observed (data not shown). Both the single-chain and the two-chain forms of intracellular Cat B were constitutively expressed with a slightly amplified staining at days 2 and 3 (Fig. 2*b*, *panels 1* and *2*). Secretion of pro-Cat L, but not of pro-Cat B, was time-dependent, whereas the mature form of Cat B was faintly increased during fibroblast differentiation (**, $p < 0.05$; Fig. 2*b*, *panels 3* and *4*). Also we observed a noteworthy TGF-β1 concentration- and time-dependent increase of membrane-bound mature Cat B (Fig. 2*c*). Most probably Cat B located in caveolae (40), because we observed by immunofluorescence an overlay with caveolin-1

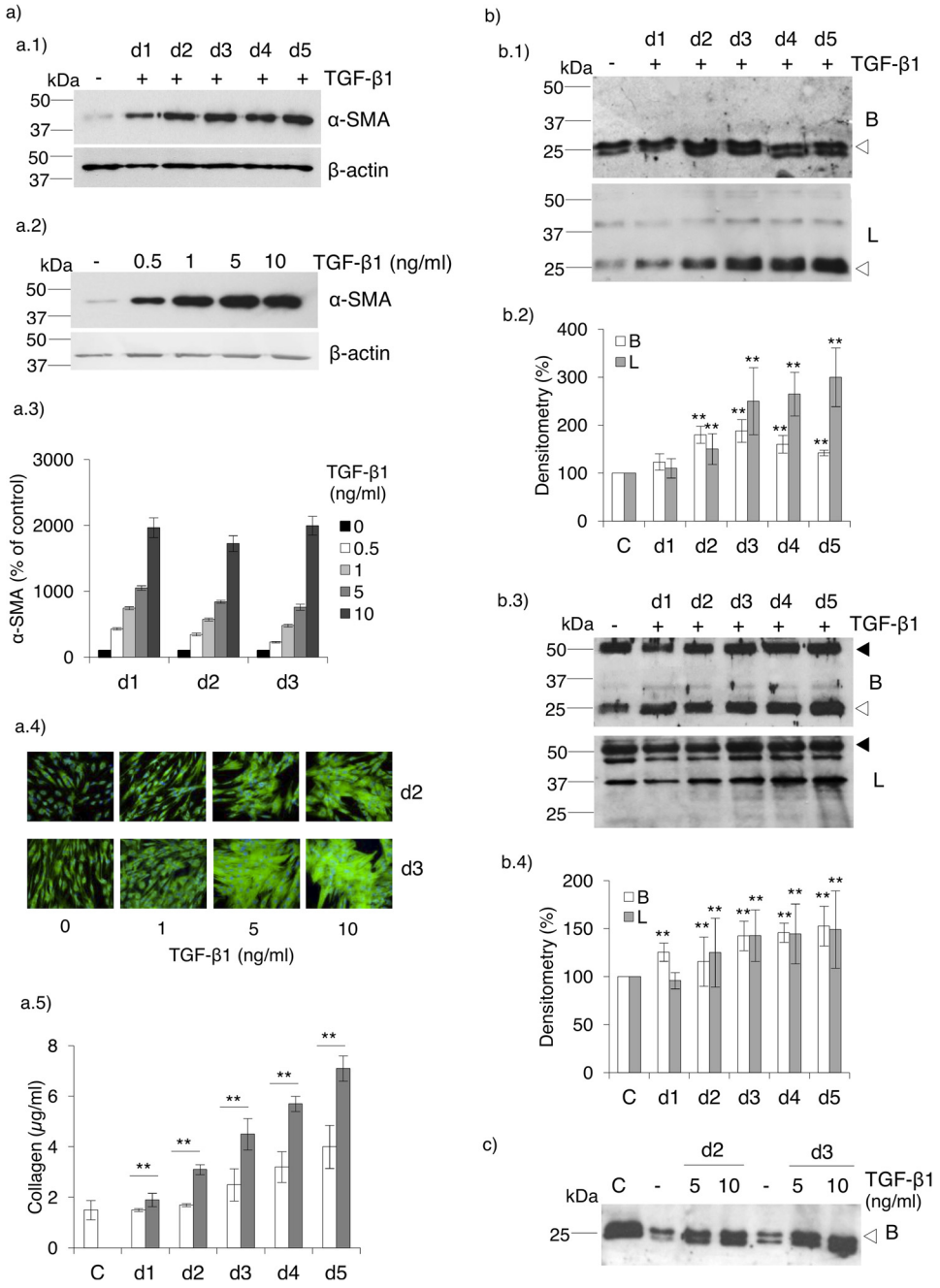

FIGURE 2. **Expression of cysteine cathepsins in CCD-19Lu human lung cell line.** *a*, validation of the CCD-19Lu fibroblast differentiation model. *Panel 1*, TGF-β1 time-dependent induction of α-SMA (Western blot analysis). *Panel 2*, TGF-β1 concentration-dependent induction of α-SMA (Western blot analysis). *Panel 3*, quantitative real time PCR analysis of α-SMA transcripts. Fibroblasts were treated by different concentrations of TGF-β1 for 3 days. The data are expressed as percentages relative to untreated control ($n = 3$). *Panel 4*, immunolabeling of α-SMA. Cells were cultured with medium or increasing concentrations of TGF-β1 for 2 and 3 days; *green* staining was performed using a specific α-SMA antibody. Nuclei were stained by DAPI (*blue*). *Panel 5*, dosage of soluble collagen in culture media (Sircol collagen assay). *White bars*, untreated fibroblasts; *gray bars*, TGF-β1-treated fibroblasts ($n = 3$; **, $p < 0.05$). *b*, human lung CCD-19Lu fibroblasts were stimulated by TGF-β1 (10 ng/ml) for 5 days. *Panel 1*, expression of intracellular Cats B and L was analyzed by Western blot. *White arrows* indicate mature forms. *Panel 2*, densitometric analysis of intracellular mature Cats B and L expression (normalized data relative to control without TGF-β1) ($n = 3$; **, $p < 0.05$). *Panel 3*, expression of extracellular pro- and mature Cats B and L was analyzed by Western blot. *Black arrows* indicate proforms of Cats, and *white arrows* indicate mature forms. *Panel 4*, densitometric analysis of extracellular (50-kDa band) pro-Cat L expression and mature Cat B (normalization relative to control without TGF-β1) ($n = 3$; **, $p < 0.05$). *c*, immunodetection of membrane-bound Cat B. CCD-19Lu cells were previously treated by 5 and 10 ng/ml of recombinant TGF-β1 for 2 and 3 days. Solubilized membrane fractions (10 μg of proteins/well) were separated by 12% SDS-PAGE under reducing conditions. *C*, control: human Cat B.

(data not shown). Expression patterns of Cats B, K, and L from cell layers of CCD-19Lu fibroblasts compared with that observed in IPF primary fibroblasts (Fig. 3*a*), although there is a difference in the intensity of immunostaining for secreted mature Cat B and pro-Cat K (Fig. 3*b*), likely because of the heterogeneous populations of fibroblasts (undifferentiated and differentiated) present in IPF explant biopsies.

Silencing of Cat B Delayed Differentiation of CCD-19Lu Fibroblasts—CCD-19Lu fibroblasts were transfected using specific siRNAs for Cats B and L as described above. Effectiveness

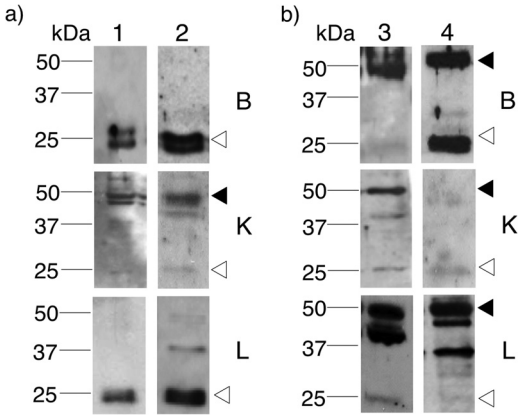

FIGURE 3. **Comparative expression of Cats B, L, and K in primary IPF fibroblasts and in CCD-19Lu fibroblasts.** Western blot analysis (day 3) was performed as previously described (see Figs. 1 and 2). *a*, lysates. *b*, culture media. *Lanes 1* and *3*, IPF fibroblasts; *lanes 2* and *4*, CCD-19Lu fibroblasts. *Black arrows* correspond to Cat proforms, and *white arrows* correspond to mature enzymes.

of the knockdown was confirmed by a reduced protein expression (Fig. 4*a*, *panel 1*). Transient silencing of Cat L had no effect on α-SMA protein and mRNA levels (Fig. 4*a*, *panels 2–4*) conversely to that reported with IPF fibroblasts. Silencing of Cat B induced a decrease of α-SMA mRNA, and Western blot analysis confirmed a minor but statistically significant impairment of α-SMA expression (densitometric analysis of normalized α-SMA/β-actin ratio; **, $p < 0.05$) (Fig. 4*a*, *panels 2–4*). Next we incubated CCD-19Lu fibroblasts in the presence of two cell permeable pharmacological inhibitors, respectively: CA-074Me (Cat B inhibitor, 10 μM, (41)) and E-64d (broad spectrum inhibitor of Cats, 50 μM). Again, a significant reduction of α-SMA expression was observed with both inhibitors (α-SMA/β-actin ratio; **, $p < 0.05$) (Fig. 4*b*, *panels 1* and *2*). Inhibitory effects of CA-074Me, the methyl ester form of CA-074, on α-SMA expression were somewhat improved, which may have partially resulted from better permeability, compared with the broad spectrum inhibitor E-64d. Nevertheless, differences between the two pharmacological drugs were not significant (Fig. 4*b*, *panel 2*). In addition, we measured the level of collagen content in culture media of myofibroblasts by Sircol assay. Although no difference was observed until day 4, a later and significant decrease of soluble collagen (days 6–8; **, $p < 0.05$) was disclosed in the presence of CA-074Me and E-64d (Fig. 4*b*, *panel 3*), which could be attributed to a delayed differentiation of fibroblasts. During TGF-β1-dependent differentiation, there was also a substantial decrease in cell layer associated collagen (average control value, 33 μg/ml) from day 6 in the presence of both Cat inhibitors (CA-074Me, average value, 17 μg/ml; E-64d, average value, 10.5 μg/ml). Although the contribution of other Cats (especially Cat L) cannot be excluded, taken together with the siRNAs experiments, the current results show that Cat B participates in TGF-β1-driven differentiation of CCD-19Lu fibroblasts and that its inhibition delays myofibrogenesis.

Previous reports have shown that TGF-β1 is activated extracellularly; in addition to plasmin, furin, MMP-2, MMP-9, MMP-13, MMP-14, chymase, and tryptase, thrombin and neutrophil elastase may be more specifically involved in the release of bioactive TGF-β1 during lung injury and pulmonary fibrosis (for review, see Refs. 42 and 43). Nevertheless complementary proteases could be also involved (44). Other studies have reported that TGF-β1, which is a glycoprotein sharing mannose 6-phosphate residues in its N-terminal proregion, could be also matured within endosomal/lysosomal compartments (45). We did not observe TGF-β1 (pro-TGF-β1 or its latent form) in the culture medium of CCD-19Lu fibroblasts; conversely, we immunodetected endogenous pro-TGF-β1 (50-kDa band) in the fraction corresponding to the cell layer (Fig. 5*a*). After pharmacological inhibition (CA-074Me) or specific silencing of Cat B, there was an accumulation of the 50-kDa band (**, $p < 0.05$; Fig. 5*b*), suggesting that Cat B is involved in the maturation of the intracellular pro-TGF-β1. Moreover, after addition of Cat B to lysates of Cat B siRNA-pretreated cell layers, both a significant increase of the mature bioactive form of TGF-β1 (25-kDa) and a decrease of the 50-kDa pro-form were observed (**, $p < 0.05$; Fig. 5, *c–e*). The release of the 25-kDa form was specifically impaired by CA-074 (**, $p < 0.05$; Fig. 5*d*). Taken together with previous data that suggest a link between the overexpression of active TGF-β1 and an upstream regulation of Cat B (20, 36, 46, 47), the present results strengthen the hypothesis that the activation of TGF-β1 may also partly depend on the proteolytic activity of intracellular Cat B. It should be noted that two additional 45- and 37-kDa bands corresponding to variant glycosylated forms of pro-TGF-β1 were observed (Fig. 5*c*) as previously reported (48). This was confirmed by an overnight treatment with endo-β-*N*-acetylglucosaminidase F1 (data not shown).

Silencing of Cat B Impaired Smad Signaling Pathway of CCD-19Lu Fibroblasts—Fibroblast Smad-induced differentiation is known to play a key role in the onset and progression of fibrosis. Abnormal Smad signaling (*i.e.* overexpression of Smads 2/3) increases the production of collagens, which hence promotes deposition of extracellular matrix proteins (49). Once phosphorylated, Smads 2 and 3 that act downstream of the TGF-β1 receptor form a complex with Co-Smad 4, which translocates to the nucleus to specifically regulate gene transcription (50). We evaluated the consequences of Cat B silencing on the Smad pathway. Although the total expression of Smads 2 and 3 was unaffected, silencing of Cat B induced a slight but significant reduction of phosphorylated Smads 2 and 3 (Fig. 6, *a* and *b*). Also TGF-β1 may activate noncanonical p38 MAPK and the JNK/SAPK family (43). Here, phosphorylation of p38 and SAPK/JNK remained unchanged (Fig. 6*c*), indicating that silencing of Cat B did not modify either signaling pathways, conversely to that observed for Smads 2 and 3 (Fig. 6*b*). The present data both verify that RNAi-mediated down-regulation of Cat B disturbed the TGF-β1-activated canonical Smad signal transduction pathway and the likely role of Cat B in driving myofibrogenesis.

Change in the Cathepsins/Cystatin C Balance during Fibroblast Differentiation—Given that the ratio cathepsins/inhibitors is disturbed in various lung diseases (22, 32, 37), we examined the balance of Cats and their natural inhibitors during fibroblast differentiation. The expression level of intracellular stefin B did not vary notably during differentiation; similarly, no significant change of the overall endopeptidase activity of Cats was detected in lysates (data not shown). This intracellular

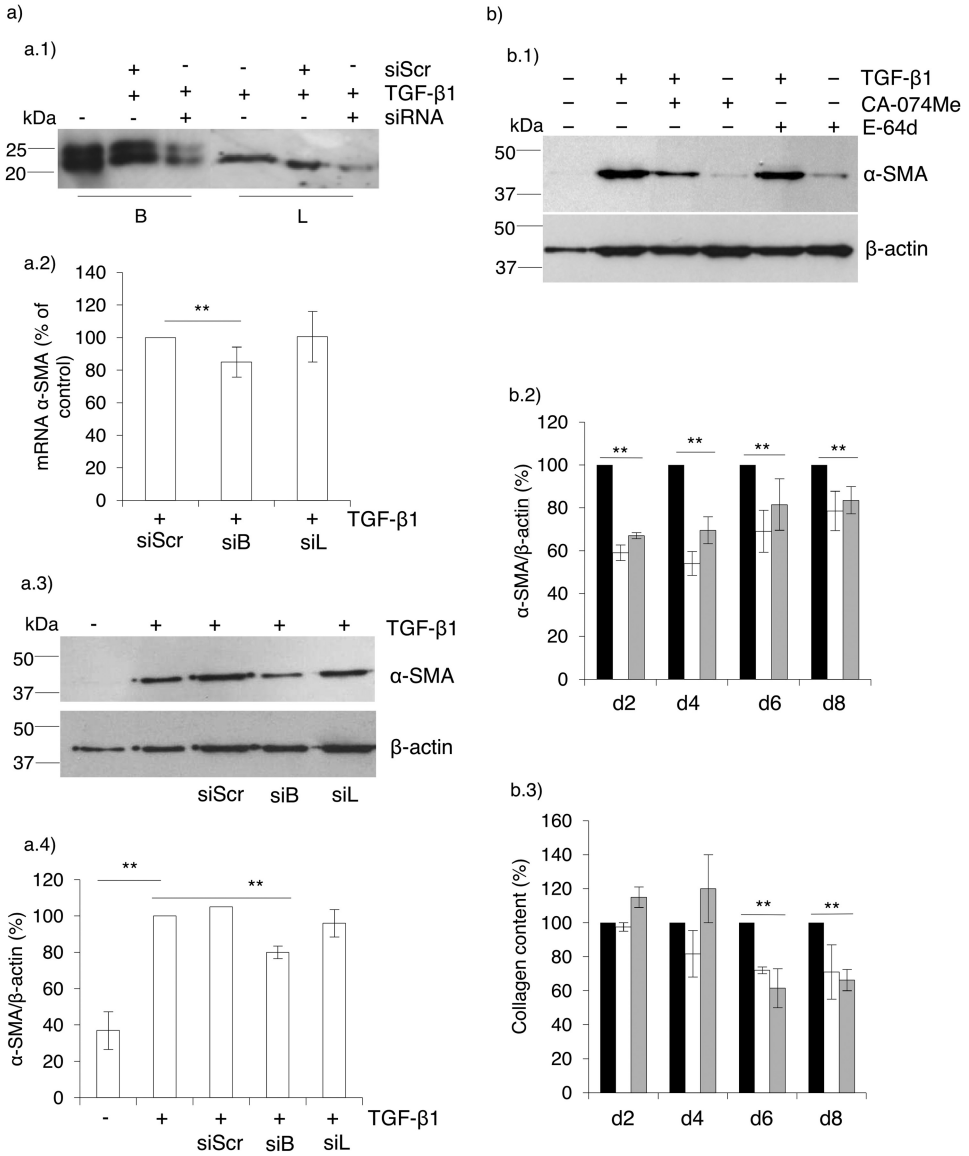

FIGURE 4. **Consequences of Cat inhibition on CCD-19Lu TGF-β1-dependent myofibrogenesis.** *a*, gene silencing of Cats. *siScr*, scrambled siRNA; *siB*, siRNA directed against Cat B; *siL*, siRNA directed against Cat L). *Panel 1*, Western blot analysis of Cat B and Cat L (representative samples). *Panel 2*, quantitative real time PCR analysis of α-SMA mRNA ($n = 3$; **, $p < 0.05$; normalized data relative to control, *i.e.* siScr treatment). *Panel 3*, at 72 h post-transfection, CCD-19Lu cell layers were lysed, and the protein level of α-SMA was analyzed by Western blot. A representative sample at day 3 is shown. *Panel 4*, densitometric analysis of three independent experiments normalized to β-actin control (**, $p < 0.05$). *b*, Cat inhibition by pharmacological inhibitors. CCD-19Lu fibroblasts were cultured with CA-074Me (10 μM) or E-64d (50 μM) 6 h before addition of TGF-β1 (10 ng/ml). *Panel 1*, Western blot analysis of α-SMA. A representative sample (day 5) is shown. *Panel 2*, densitometric analysis (normalized values relative to β-actin loading control) ($n = 3$; **, $p < 0.05$). *Panel 3*, dosage of soluble collagen in culture media (Sircol assay). Experiments were done in the presence of TGF-β1 (10 ng/ml). *Black bars*, TGF-β1-treated control; *white bars*, TGF-β1+CA-074Me; *gray bars*, TGF-β1+E-64d ($n = 3$; **, $p < 0.05$).

activity was mostly Cat B-dependent because it was inhibited (~80%) by CA-074. On the other hand, no detectable cathepsin activity was found in culture media, in contrast with that observed with macrophages and smooth muscle cells (51–53). Western blot analysis indicated the presence of extracellular cystatin C (~13 kDa) that increased during TGF-β1-dependent differentiation of CCD-19Lu fibroblasts (Fig. 7*a*). Conversely the mRNA level of cystatin C remained unchanged following a pretreatment with actinomycin D, suggesting that cystatin C was not transcriptionally regulated during differentiation as previously observed for Cats B, K, and L (data not shown). The addition of brefeldin A abolished the appearance of extracellular cystatin C, supporting that TGF-β1 governed the up-regulation of cystatin C secretion (Fig. 7*b*). A similar up-regulation was reported for human vascular smooth muscle cells (53), for profibrogenic hepatic stellate cells (54), and also during oral submucous fibrosis (55). The induction of secretion was confirmed by an enzyme-linked immunosorbent assay. At day 3, the cystatin C concentration raised ~5-fold in the presence of TGF-β1 (4 ng/ml *versus* 22 ng/ml; $p < 0.001$) (Fig. 7*c*). In conjunction with cystatin C ELISA, a noteworthy increase of Cat inhibitory capacity was observed by measuring the ability of fibroblast culture media to inhibit exogenous E-64-titrated papain ($p < 0.05$) (Fig. 7*d*). In a similar way, in a rat model of bleomycin-induced lung fibrosis, the protease/antiprotease ratio was shifted in favor of Cat inhibitors in the alveolar lumen

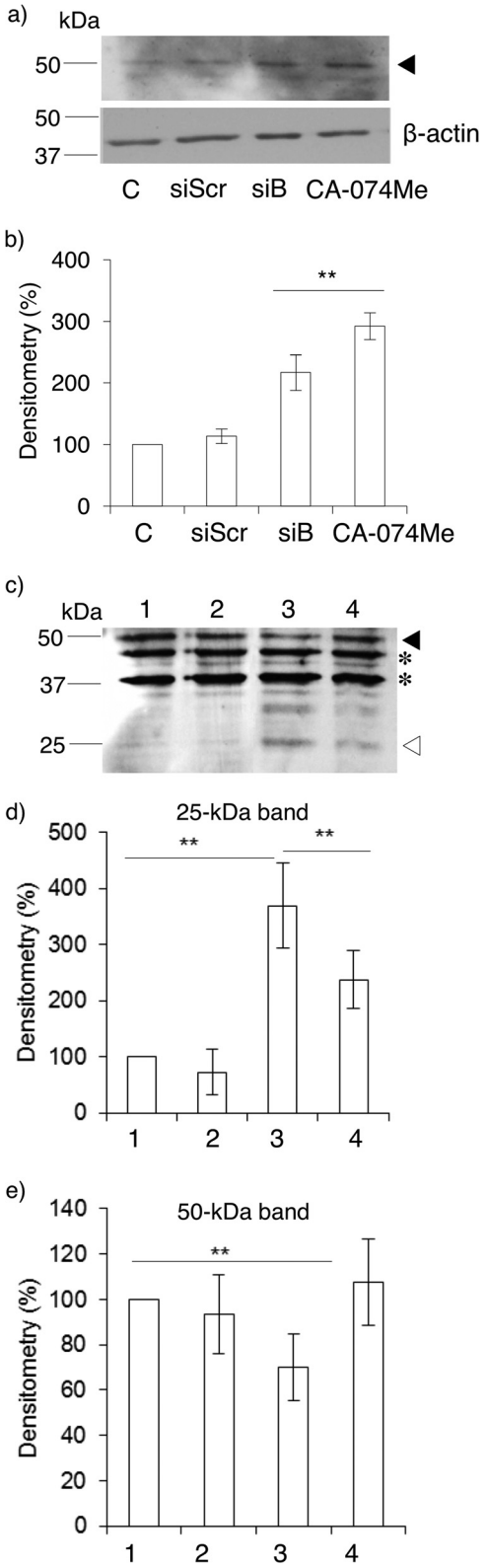

FIGURE 5. **Maturation of TGF-β1 by Cat B.** Western blot analysis of intracellular TGF-β1 expression (representative samples) is shown. *a*, CCD-19Lu cells were transfected with siRNA directed against Cat B (*siB*) or scrambled siRNA (*siScr*). Twenty-four hours later, fibroblasts were treated by 10 ng/ml of recombinant TGF-β1 for 2 days. In parallel, pharmacological inhibition of Cat B was performed by the addition of CA-074Me (10 μM) 6 h prior to the TGF-β1 stimulation. *b*, corresponding densitometric analysis of the intracellular 50-kDa pro-TGF-β1 ($n = 3$; **, $p < 0.05$). *c*, lysates of fibroblasts pretreated by Cat B siRNA were incubated with Cat B (1 μM) for 3 h at 30 °C. Proteolysis products were separated by SDS-PAGE under reducing conditions (10 μg of proteins/well). *Lane 1*, 0 h (control); *lane 2*, 3 h (control); *lane 3*, 3-h incubation with Cat B; *lane 4*, 3-h incubation with CA-074-inactivated Cat B. *Black arrow*, 50-kDa band (pro-TGF-β1); *white arrow*, 25-kDa band (TGF-β1); *asterisks*, 45- and 37-kDa bands corresponding to variant glycosylated forms of pro-TGF-β1). *d*, densitometric analysis of the 25-kDa band ($n = 3$; **, $p < 0.05$). *e*, densitometric analysis of the 50-kDa band ($n = 3$; **, $p < 0.05$).

and BALFs (56). Taken together with the imbalance in the expression of Cats and cystatin C in favor of inhibition and the fact that Cats are potent enzymes that participate in the degradation of the major components of the extracellular matrix (*e.g.* collagens and fibronectin) and its remodeling, the present data suggest that TGF-β1 may also drive fibrogenesis by up-regulating secretion of cystatin C that sequentially promotes inhibition of extracellular Cats. We tested the hypothesis by transfection of CCD19-Lu fibroblasts by silencing of cystatin C. Effectiveness of the transient knockdown by siRNA was confirmed by a critical reduction of immunoreactive secreted cystatin C (Fig. 7*e*). Subsequently, we assessed the consequence of cystatin C silencing on extracellular Cat activities by using an irreversible probe (Biotinyl-$(PEG)_2$-LVG-DMK) that targets the nucleophilic active site thiol of cysteine cathepsins. Labeling of active Cats was restored when cystatin C was inhibited by specific siRNA (Fig. 7*f*). Accordingly proteolytic activity that was broadly inhibited by CA-074 (data not shown) and thus predominantly corresponding to Cat B was retrieved in culture media ($p < 0.001$) (Fig. 7*g*). Analogous experiments were performed with human primary IPF fibroblasts. We detected a similar level of extracellular cystatin C in IPF samples both incubated in the presence or absence of TGF-β1 (Fig. 8*a*), which is in good agreement with the fact that a noticeable amount of IPF fibroblasts were already differentiated into myofibroblasts (57). Also, secretion of cystatin C was abolished by addition of brefeldin A (Fig. 8*a*). Conversely to that observed for CCD-19Lu myofibroblasts, we detected Cat activity in IPF culture media. This residual proteolytic activity of IPF samples obtained from lung biopsies probably relied on the presence (in addition to fibroblastic cells) of some resident macrophages and epithelial cells that are the primary source of extracellular Cats (8, 22, 58, 59). Nevertheless, as observed for the CCD-19Lu model, inhibition of cystatin C by siRNA drastically rescued (4–5-fold) Cat B activity ($p < 0.001$) (Fig. 8*b*), supporting our hypothesis that secreted cystatin C allows control of the enzymatic activity of extracellular Cats.

DISCUSSION

Fibrotic disorders are associated with a dysregulation of proteolytic activities, and there are increasing indications that cysteine cathepsins might be involved. For example, inhibition of murine Cat B diminished hepatic inflammation and fibrogenesis (19). Also, expression of Cat B is increased during differentiation of stellate cells, and data support that Cat B participates in liver fibrogenesis (20). Alternatively, the inhibition of Cat S may impair the TGF-β1-dependent differentiation of cardiac fibroblasts in a model of myocardial infarction (21). Some apparently conflicting results were reported for lung fibrosis. Overexpression of Cat K has been reported in a murine model of bleomycin-induced lung fibrosis, whereas Cat K deficiency

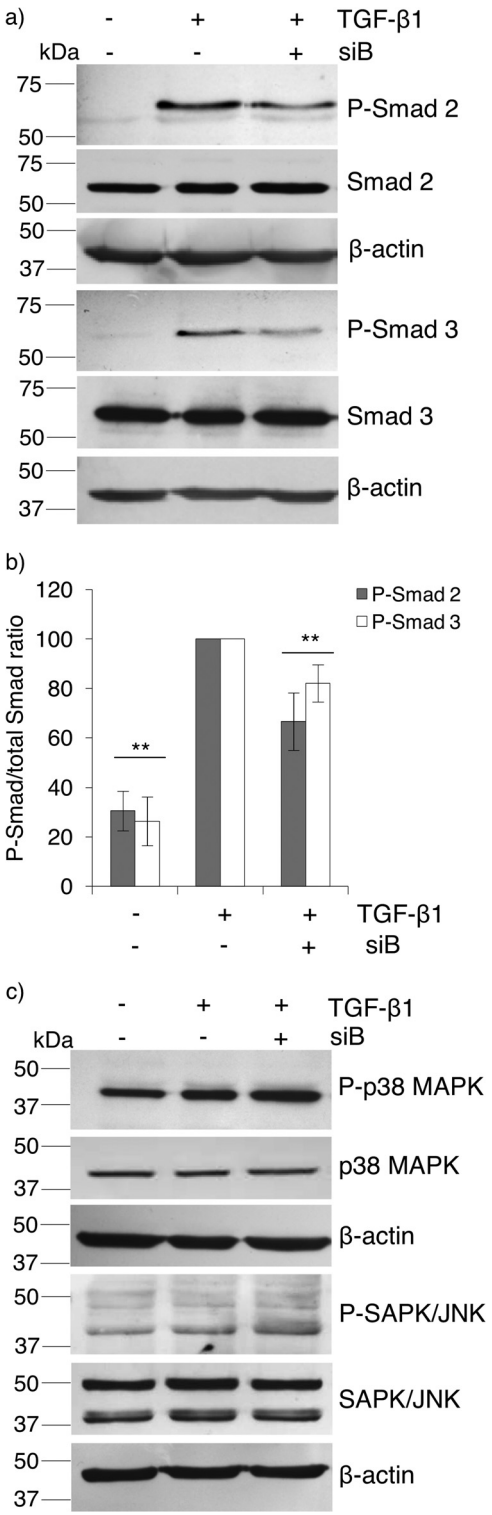

FIGURE 6. **Consequence of Cat B silencing on TGF-β1 signaling pathways.** At 24 h post-transfection, CCD-19Lu cells were stimulated with recombinant TGF-β1 (10 ng/ml) for 1 h. Lysates were then subjected to SDS-PAGE under reducing conditions. *a*, immunoblot of endogenous phospho-Smad 2 and phospho-Smad 3 (P-Smad 2 and P-Smad 3) and total Smad 2 and Smad 3 expression. *b*, densitometric analysis (normalization: phosphorylated/total protein ratio). *Gray bars*, P-Smad-2; *white bars*, P-Smad-3, ($n = 3$; **, $p < 0.05$). *c*, immunoblot of phospho kinases (P-p38 MAPK and P-SAPK/JNK) and total kinases (p38 MAPK and SAPK/JNK). *siB*, Cat B siRNA.

exacerbated lung fibrosis (25). Moreover, TGF-β1 down-regulates both Cat K expression in fibroblasts favoring silica-induced lung fibrosis in mice (27). However, whether human Cats may directly drive lung fibroblast differentiation or whether cystatins, their endogenous natural inhibitors, may regulate their fibrogenic potential has not been specifically addressed to date. To achieve this goal, we developed an experimental model of differentiated CCD-19Lu fibroblasts and also used primary fibroblasts obtained by biopsies from IPF patients.

First, we characterized Cats expressed by IPF fibroblasts. Mature Cat L and Cat B were detected in cell lysates, whereas secreted Cats B and L were predominantly found as zymogens. On the other hand, during differentiation of lung CCD-19Lu fibroblasts, we observed that secreted Cat B was present as both pro- and mature forms, whereas we did not detect mature extracellular Cat L in culture media. According to these observations, mature Cat B, but not Cat L, may be recruited out of late endosomes/lysosomes, transported to the plasma membrane, and secreted into the extracellular space by CCD-19Lu cells, whereas transport along the secretory pathway and secretion of both pro-Cat L and pro-Cat B may occur, as reviewed by Brix *et al.* (13).

We observed that silencing of Cats B or L induced a reduction of α-SMA expression, supporting that both proteases may be involved in TGF-β1-driven differentiation of primary IPF fibroblasts. Of interest, esophageal keratinocytes activate fibroblasts through the secretion of TGF-β1, which may be activated by Cat B during esophageal cancer (60). Similarly, invasion of melanoma cells is prompted by stromal fibroblasts in a way that is associated with both TGF-β1 activation and Cats B and L activities (61). Also, TGF-β1 might be activated through a process initiated by Cat B (62). On the other hand, silencing of Cat B, but not Cat L, had a significant effect on α-SMA protein and mRNA levels during differentiation of CCD-19Lu cells. This apparent discrepancy associated with Cat L silencing between CCD-19Lu and IPF fibroblasts probably relies on the fact that CCD-19Lu fibroblasts correspond to a homogenous cell line at variance with primary IPF fibroblasts that were obtained from lung biopsies and corresponded to a heterogeneous population including already differentiated myofibroblasts (57). Similar results were observed in the presence of CA-074Me or E-64d. Although measurement of the residual peptidase activity in lysates support that CA-074Me inhibited primarily intracellular Cat B, the possibility that CA-074Me may also interfere and partly inactivate lysosomal Cat L within fibroblasts cannot be excluded as previously reported (63). Nevertheless current results sustain that Cat B participates in TGF-β1-driven differentiation of CCD-19Lu fibroblasts and its inhibition delays myofibrogenesis. In addition to various proteases that are involved in the extracellular activation of TGF-β1 (see for review Refs. 42 and 43), it has been proposed that other enzymes could participate in the release of bioactive TGF-β1 during lung injury and pulmonary fibrosis (44). Interestingly, TGF-β1 is a glycoprotein that shares mannose 6-phosphate residues in its N-terminal proregion, thus allowing its delivery to endosomal/lysosomal compartments (45). Moreover, previous data have suggested a connection between the overexpression of active TGF-β1 and an upstream regulation of Cat B (20,

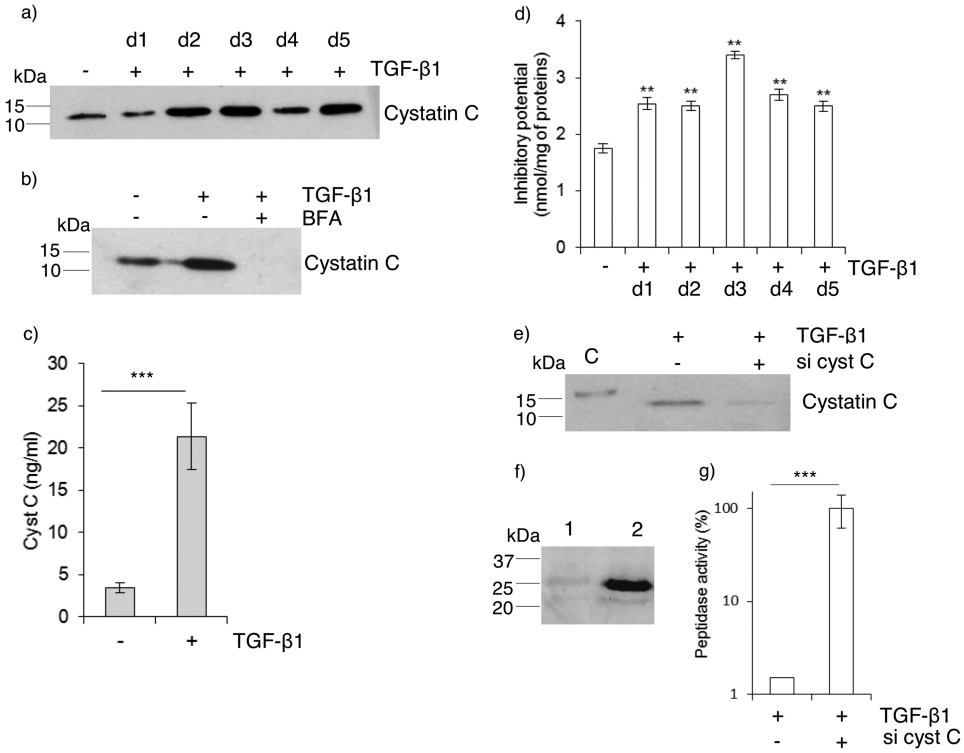

FIGURE 7. **TGF-β1-driven secretion of cystatin C by CCD-19Lu cells.** Experiments were conducted in the presence of TGF-β1 (10 ng/ml). *a*, Western blot analysis of extracellular cystatin C. *b*, extracellular cystatin C level after treatment with BFA (0.5 μg/ml). A representative sample (day 3) is shown. *c*, dosage of secreted cystatin C (ELISA DuoSet) ($n = 3$; ***, $p < 0.001$). *d*, inhibitory potential of myofibroblast culture media, expressed as inhibitory site (cystatin-like) equivalent ($n = 3$; **, $p < 0.05$). *e*, Western blot analysis of secreted cystatin C after gene silencing. *C*, recombinant cystatin C (the recombinant form has an additional C-terminal 10 His tag; apparent molecular mass of 17 kDa). *si cyst C*, cystatin C siRNA. *f*, active site labeling of extracellular Cats by Biotinyl-$(PEG)_2$-LVG-DMK. *Lane 1*, TGF-β1 treated control cells; *lane 2*, cystatin C siRNA. *g*, recovery of extracellular peptidase activity of Cats after silencing of cystatin C ($n = 3$; ***, $p < 0.001$) (substrate: Z-Phe-Arg-AMC).

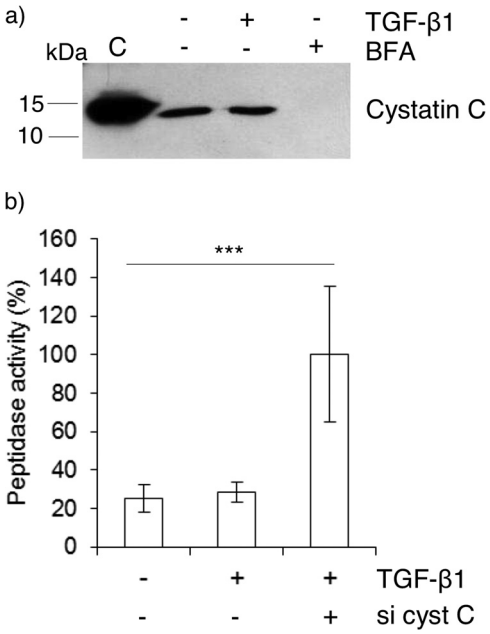

FIGURE 8. **Secretion of cystatin C by primary IPF fibroblasts.** *a*, Western blot analysis of secreted cystatin C in the presence or absence of BFA (0. 5 μg/ml) at day 3. *C*, recombinant cystatin C. *b*, endopeptidase activity of extracellular Cats ($n = 3$; ***, $p < 0.001$) (substrate: Z-Phe-Arg-AMC).

36, 46, 47). Here we observed that both pharmacological inhibition and specific silencing of Cat B led to the intracellular accumulation of pro-TGF-β1 (50-kDa form). Alternatively addition of exogenous Cat B to lysates of Cat B siRNA-pretreated fibroblasts conducted to the increase of the 25-kDa bioactive TGF-β1. Also down-regulation of Cat B disturbed the TGF-β1-activated Smad signal transduction pathway. Taken together, the present results strengthen the hypothesis that the activation of TGF-β1 also partly depends on the proteolytic activity of intracellular Cat B.

Also we established that secretion of cystatin C increased during differentiation of lung fibroblasts. Subsequently cystatin C participated in the control of extracellular Cats, because its gene silencing restored their proteolytic activities, which support the possibility that TGF-β1-dependent secretion of cystatin C may finely tune promotion of fibrosis by inhibiting Cats that are potent ECM-degrading enzymes. In support of this hypothesis, it is known that the myocardial fibrosis often associated with heart failure results from modifications in ECM proteins secreted by fibroblasts. As shown in an earlier report, exposure of cardiac fibroblasts to exogenous cystatin C resulted in the inhibition of Cat B and accumulation of fibronectin and collagens (64). Conversely, during lung inflammations associated with widespread ECM breakdown, the BALFs cathepsin/cystatin ratio was reversed in favor of uncontrolled proteolysis (8, 22).

In summary, we propose that intracellular Cat B participates in the TGF-β1-driven differentiation of lung fibroblasts via the intracellular processing of the 50-kDa pro-TGF-β1 to its 25-kDa mature form (Fig. 9). Subsequently, secreted TGF-β1

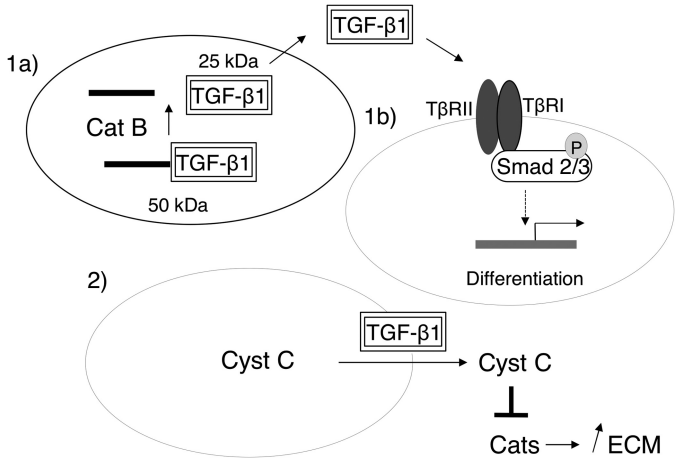

FIGURE 9. **Involvement of Cat B and cystatin C in TGF-β1-driven differentiation of lung fibroblasts.** We propose that lysosomal Cat B may participate in the intracellular proteolytic activation of TGF-β1 (*step 1a*) and that bioactive TGF-β1 binds to its specific receptors and triggers Smad 2/3 phosphorylation and myodifferentiation of lung fibroblasts (*step 1b*). In addition, TGF-β1 up-regulates secretion of cystatin C (*step 2*). Subsequently, the cystatin C-dependent inhibition of ECM-degrading Cats may favor collagen deposition and promote fibrosis.

triggers the canonical Smad signaling pathway, thus initiating myofibrogenesis. Moreover, we establish that during myodifferentiation, TGF-β1 up-regulates the secretion of cystatin C, allowing inhibition of extracellular Cats. According to previous reports (24, 25), we can hypothesize that impairment of the Cat-dependent proteolytic activities then favors excessive accumulation of collagens and ultimately ECM deposition in lung. Interestingly, we have recently proposed that human cystatin C could be a specific biomarker of lung fibrosis because its protein level is critically increased in IPF BALFs compared with non-IPF BALFs ($p < 0.001$) (65). Finally, present data support that both cysteine cathepsins and cystatin C, their related tight binding inhibitor, could play a crucial role in myofibrogenesis and the progression of lung fibrosis.

Acknowledgment—We thank Dr. Emmanuelle Liaudet-Coopman (Institut de Recherche en Cancérologie de Montpellier (IRCM), Inserm U896, Montpellier, France) for the kind gift of anti-Smad and anti-JNK antibodies.

REFERENCES

1. Bjoraker, J. A., Ryu, J. H., Edwin, M. K., Myers, J. L., Tazelaar, H. D., Schroeder, D. R., and Offord, K. P. (1998) Prognostic significance of histopathologic subsets in idiopathic pulmonary fibrosis. *Am. J. Respir. Crit. Care Med.* **157,** 199–203
2. Raghu, G., Freudenberger, T. D., Yang, S., Curtis, J. R., Spada, C., Hayes, J., Sillery, J. K., Pope, C. E., and Pellegrini, C. A. (2006) High prevalence of abnormal acid gastro-oesophageal reflux in idiopathic pulmonary fibrosis. *Eur. Respir. J.* **27,** 136–142
3. Adamali, H. I., and Maher, T. M. (2012) Current and novel drug therapies for idiopathic pulmonary fibrosis. *Drug Des. Devel. Ther.* **6,** 261–271
4. Border, W. A., and Noble, N. A. (1994) Transforming growth factor beta in tissue fibrosis. *N. Engl. J. Med.* **331,** 1286–1292
5. Khalil, N., Parekh, T., O'Connor, R., Antman, N., Kepron, W., Yehaualaeshet, T., Xu, Y., and Gold, L. (2001) Regulation of the effects of TGF-β1 by activation of latent TGF-β1 and differential expression of TGF-β receptors (TβR-I and TβR-II) in idiopathic pulmonary fibrosis. *Thorax* **56,** 907–915
6. Hinz, B., Phan, S. H., Thannickal, V. J., Galli, A., Bochaton-Piallat, M.-L., and Gabbiani, G. (2007) The myofibroblast: one function, multiple origins. *Am. J. Pathol.* **170,** 1807–1816
7. Desmoulière, A., Geinoz, A., Gabbiani, F., and Gabbiani, G. (1993) Transforming growth factor-beta 1 induces alpha-smooth muscle actin expression in granulation tissue myofibroblasts and in quiescent and growing cultured fibroblasts. *J. Cell Biol.* **122,** 103–111
8. Kasabova, M., Saidi, A., Naudin, C., Sage, J., Lecaille, F., and Lalmanach, G. (2011) Cysteine Cathepsins: Markers and Therapy Targets in Lung Disorders. *Clin. Rev. Bone Miner. Metab.* **9,** 148–161
9. Lecaille, F., Kaleta, J., and Brömme, D. (2002) Human and parasitic papain-like cysteine proteases: their role in physiology and pathology and recent developments in inhibitor design. *Chem. Rev.* **102,** 4459–4488
10. Novinec, M., and Lenarčič, B. (2013) Cathepsin K: a unique collagenolytic cysteine peptidase. *Biol. Chem.* **394,** 1163–1179
11. Rawlings, N. D., Barrett, A. J., and Bateman, A. (2012) MEROPS: the database of proteolytic enzymes, their substrates and inhibitors. *Nucleic Acids Res.* **40,** D343-D350
12. Turk, V., Stoka, V., Vasiljeva, O., Renko, M., Sun, T., Turk, B., and Turk, D. (2012) Cysteine cathepsins: from structure, function and regulation to new frontiers. *Biochim. Biophys. Acta* **1824,** 68–88
13. Brix, K., Dunkhorst, A., Mayer, K., and Jordans, S. (2008) Cysteine cathepsins: cellular roadmap to different functions. *Biochimie (Paris)* **90,** 194–207
14. Reiser, J., Adair, B., and Reinheckel, T. (2010) Specialized roles for cysteine cathepsins in health and disease. *J. Clin. Invest.* **120,** 3421–3431
15. Turk, B. (2006) Targeting proteases: successes, failures and future prospects. *Nat. Rev. Drug Discov.* **5,** 785–799
16. Vasiljeva, O., Reinheckel, T., Peters, C., Turk, D., Turk, V., and Turk, B. (2007) Emerging roles of cysteine cathepsins in disease and their potential as drug targets. *Curr. Pharm. Des.* **13,** 387–403
17. Abrahamson, M., Alvarez-Fernandez, M., and Nathanson, C.-M. (2003) Cystatins. *Biochem. Soc. Symp.* 179–199
18. Turk, V., Stoka, V., and Turk, D. (2008) Cystatins: biochemical and structural properties, and medical relevance. *Front. Biosci.* **13,** 5406–5420
19. Canbay, A., Guicciardi, M. E., Higuchi, H., Feldstein, A., Bronk, S. F., Rydzewski, R., Taniai, M., and Gores, G. J. (2003) Cathepsin B inactivation attenuates hepatic injury and fibrosis during cholestasis. *J. Clin. Invest.* **112,** 152–159
20. Moles, A., Tarrats, N., Fernández-Checa, J. C., and Marí, M. (2009) Cathepsins B and D drive hepatic stellate cell proliferation and promote their fibrogenic potential. *Hepatology* **49,** 1297–1307
21. Chen, H., Wang, J., Xiang, M.-X., Lin, Y., He, A., Jin, C.-N., Guan, J., Sukhova, G. K., Libby, P., Wang, J.-A., and Shi, G.-P. (2013) Cathepsin S-mediated fibroblast trans-differentiation contributes to left ventricular remodelling after myocardial infarction. *Cardiovasc. Res.* **100,** 84–94
22. Lalmanach, G., Diot, E., Godat, E., Lecaille, F., and Hervé-Grépinet, V. (2006) Cysteine cathepsins and caspases in silicosis. *Biol. Chem.* **387,** 863–870
23. Quinn, D. J., Weldon, S., and Taggart, C. C. (2010) Antiproteases as therapeutics to target inflammation in cystic fibrosis. *Open Respir. Med. J.* **4,** 20–31
24. Bühling, F., Röcken, C., Brasch, F., Hartig, R., Yasuda, Y., Saftig, P., Brömme, D., and Welte, T. (2004) Pivotal role of cathepsin K in lung fibrosis. *Am. J. Pathol.* **164,** 2203–2216
25. Zhang, D., Leung, N., Weber, E., Saftig, P., and Brömme, D. (2011) The effect of cathepsin K deficiency on airway development and TGF-β1 degradation. *Respir. Res.* **12,** 72
26. Zhang, D., Huang, C., Yang, C., Liu, R. J., Wang, J., Niu, J., and Bromme, D. (2011) Antifibrotic effects of curcumin are associated with overexpression of cathepsins K and L in bleomycin treated mice and human fibroblasts. *Respir. Res.* **12,** 154
27. Van den Brûle, S., Misson, P., Bühling, F., Lison, D., and Huaux, F. (2005) Overexpression of cathepsin K during silica-induced lung fibrosis and control by TGF-beta. *Respir. Res.* **6,** 84
28. Gerber, A., Wille, A., Welte, T., Ansorge, S., and Bühling, F. (2001) Interleukin-6 and transforming growth factor-beta 1 control expression of cathepsins B and L in human lung epithelial cells. *J. Interf. Cytokine Res.* **21,** 11–19

29. Lalmanach, G., Mayer, R., Serveau, C., Scharfstein, J., and Gauthier, F. (1996) Biotin-labelled peptidyl diazomethane inhibitors derived from the substrate-like sequence of cystatin: targeting of the active site of cruzipain, the major cysteine proteinase of Trypanosoma cruzi. *Biochem. J.* **318,** 395–399
30. Akamine, A., Raghu, G., and Narayanan, A. S. (1992) Human lung fibroblast subpopulations with different C1q binding and functional properties. *Am. J. Respir. Cell Mol. Biol.* **6,** 382–389
31. Zi, Z., Feng, Z., Chapnick, D. A., Dahl, M., Deng, D., Klipp, E., Moustakas, A., and Liu, X. (2011) Quantitative analysis of transient and sustained transforming growth factor-β signaling dynamics. *Mol. Syst. Biol.* **7,** 492
32. Serveau-Avesque, C., Ferrer-di Martino, M., Hervé-Grépinet, V., Hazouard, E., Gauthier, F., Diot, E., and Lalmanach, G. (2006) Active cathepsins B, H, K, L and S in human inflammatory bronchoalveolar lavage fluids. *Biol. Cell* **98,** 15–22
33. Assfalg-Machleidt, I., Billing, A., Fröhlich, D., Nast-Kolb, D., Joka, T., Jochum, M., and Machleidt, W. (1992) The role of the kininogens as cysteine proteinase inhibitors in local and systemic inflammation. *Agents Actions. Suppl.* **38,** 312–321
34. Florent, I., Lecaille, F., Montagne, J.-J., Gauthier, F., Schrével, J., and Lalmanach, G. (2005) Labelling of four distinct trophozoite falcipains of Plasmodium falciparum by a cystatin-derived probe. *Biol. Chem.* **386,** 401–406
35. Srivastava, M., Steinwede, K., Kiviranta, R., Morko, J., Hoymann, H.-G., Länger, F., Buhling, F., Welte, T., and Maus, U. A. (2008) Overexpression of cathepsin K in mice decreases collagen deposition and lung resistance in response to bleomycin-induced pulmonary fibrosis. *Respir. Res.* **9,** 54
36. Moles, A., Tarrats, N., Fernández-Checa, J. C., and Marí, M. (2012) Cathepsin B overexpression due to acid sphingomyelinase ablation promotes liver fibrosis in Niemann-Pick disease. *J. Biol. Chem.* **287,** 1178–1188
37. Perdereau, C., Godat, E., Maurel, M.-C., Hazouard, E., Diot, E., and Lalmanach, G. (2006) Cysteine cathepsins in human silicotic bronchoalveolar lavage fluids. *Biochim. Biophys. Acta* **1762,** 351–356
38. Naudin, C., Joulin-Giet, A., Couetdic, G., Plésiat, P., Szymanska, A., Gorna, E., Gauthier, F., Kasprzykowski, F., Lecaille, F., and Lalmanach, G. (2011) Human cysteine cathepsins are not reliable markers of infection by Pseudomonas aeruginosa in cystic fibrosis. *PLoS ONE* **6,** e25577
39. Takeyabu, K., Betsuyaku, T., Nishimura, M., Yoshioka, A., Tanino, M., Miyamoto, K., and Kawakami, Y. (1998) Cysteine proteinases and cystatin C in bronchoalveolar lavage fluid from subjects with subclinical emphysema. *Eur. Respir. J.* **12,** 1033–1039
40. Jane, D. T., Morvay, L., Dasilva, L., Cavallo-Medved, D., Sloane, B. F., and Dufresne, M. J. (2006) Cathepsin B localizes to plasma membrane caveolae of differentiating myoblasts and is secreted in an active form at physiological pH. *Biol. Chem.* **387,** 223–234
41. Buttle, D. J., Murata, M., Knight, C. G., and Barrett, A. J. (1992) CA074 methyl ester: a proinhibitor for intracellular cathepsin B. *Arch. Biochem. Biophys.* **299,** 377–380
42. Jenkins, G. (2008) The role of proteases in transforming growth factor-beta activation. *Int. J. Biochem. Cell Biol.* **40,** 1068–1078
43. Biernacka, A., Dobaczewski, M., and Frangogiannis, N. G. (2011) TGF-β signaling in fibrosis. *Growth Factors* **29,** 196–202
44. Daley, W. P., Peters, S. B., and Larsen, M. (2008) Extracellular matrix dynamics in development and regenerative medicine. *J. Cell Sci.* **121,** 255–264
45. Purchio, A. F., Cooper, J. A., Brunner, A. M., Lioubin, M. N., Gentry, L. E., Kovacina, K. S., Roth, R. A., and Marquardt, H. (1988) Identification of mannose 6-phosphate in two asparagine-linked sugar chains of recombinant transforming growth factor-beta 1 precursor. *J. Biol. Chem.* **263,** 14211–14215
46. Somanna, A., Mundodi, V., and Gedamu, L. (2002) Functional analysis of cathepsin B-like cysteine proteases from Leishmania donovani complex. Evidence for the activation of latent transforming growth factor beta. *J. Biol. Chem.* **277,** 25305–25312
47. Gogineni, V. R., Gupta, R., Nalla, A. K., Velpula, K. K., and Rao, J. S. (2012) uPAR and cathepsin B shRNA impedes TGF-β1-driven proliferation and invasion of meningioma cells in a XIAP-dependent pathway. *Cell Death Dis.* **3,** e439
48. Brunner, A. M., Gentry, L. E., Cooper, J. A., and Purchio, A. F. (1988) Recombinant type 1 transforming growth factor beta precursor produced in Chinese hamster ovary cells is glycosylated and phosphorylated. *Moll. Cell Biol.* **8,** 2229–2232
49. Gauldie, J., Kolb, M., Ask, K., Martin, G., Bonniaud, P., and Warburton, D. (2006) Smad3 signaling involved in pulmonary fibrosis and emphysema. *Proc. Am. Thorac. Soc.* **3,** 696–702
50. Shi, Y., and Massagué, J. (2003) Mechanisms of TGF-beta signaling from cell membrane to the nucleus. *Cell* **113,** 685–700
51. Reddy, V. Y., Zhang, Q. Y., and Weiss, S. J. (1995) Pericellular mobilization of the tissue-destructive cysteine proteinases, cathepsins B, L, and S, by human monocyte-derived macrophages. *Proc. Natl. Acad. Sci. U.S.A.* **92,** 3849–3853
52. Sukhova, G. K., Shi, G. P., Simon, D. I., Chapman, H. A., and Libby, P. (1998) Expression of the elastolytic cathepsins S and K in human atheroma and regulation of their production in smooth muscle cells. *J. Clin. Invest.* **102,** 576–583
53. Shi, G.-P., Sukhova, G. K., Grubb, A., Ducharme, A., Rhode, L. H., Lee, R. T., Ridker, P. M., Libby, P., and Chapman, H. A. (1999) Cystatin C deficiency in human atherosclerosis and aortic aneurysms. *J. Clin. Invest.* **104,** 1191–1197
54. Gressner, A. M., Lahme, B., Meurer, S. K., Gressner, O., and Weiskirchen, R. (2006) Variable expression of cystatin C in cultured trans-differentiating rat hepatic stellate cells. *World J. Gastroenterol.* **12,** 731–738
55. Chung-Hung, T., Shun-Fa, Y., and Yu-Chao, C. (2007) The upregulation of cystatin C in oral submucous fibrosis. *Oral Oncol.* **43,** 680–685
56. Koslowski, R., Knoch, K., Kuhlisch, E., Seidel, D., and Kasper, M. (2003) Cathepsins in bleomycin-induced lung injury in rat. *Eur. Respir. J.* **22,** 427–435
57. Gabbiani, G. (2003) The myofibroblast in wound healing and fibrocontractive diseases. *J. Pathol.* **200,** 500–503
58. Heidtmann, H. H., Salge, U., Havemann, K., Kirschke, H., and Wiederanders, B. (1993) Secretion of a latent, acid activatable cathepsin L precursor by human non-small cell lung cancer cell lines. *Oncol. Res.* **5,** 441–451
59. Bühling, F., Gerber, A., Häckel, C., Krüger, S., Köhnlein, T., Brömme, D., Reinhold, D., Ansorge, S., and Welte, T. (1999) Expression of cathepsin K in lung epithelial cells. *Am. J. Respir. Cell Mol. Biol.* **20,** 612–619
60. Andl, C. D., McCowan, K. M., Allison, G. L., and Rustgi, A. K. (2010) Cathepsin B is the driving force of esophageal cell invasion in a fibroblast-dependent manner. *Neoplasia* **12,** 485–498
61. Yin, M., Soikkeli, J., Jahkola, T., Virolainen, S., Saksela, O., and Hölttä, E. (2012) TGF-β Signaling, Activated Stromal Fibroblasts, and Cysteine Cathepsins B and L Drive the Invasive Growth of Human Melanoma Cells. *Am. J. Pathol.* **181,** 2202–2216
62. Guo, M., Mathieu, P. A., Linebaugh, B., Sloane, B. F., and Reiners, J. J., Jr (2002) Phorbol ester activation of a proteolytic cascade capable of activating latent transforming growth factor-betaL a process initiated by the exocytosis of cathepsin B. *J. Biol. Chem.* **277,** 14829–14837
63. Montaser, M., Lalmanach, G., and Mach, L. (2002) CA-074, but not its methyl ester CA-074Me, is a selective inhibitor of cathepsin B within living cells. *Biol. Chem.* **383,** 1305–1308
64. Xie, L., Terrand, J., Xu, B., Tsaprailis, G., Boyer, J., and Chen, Q. M. (2010) Cystatin C increases in cardiac injury: a role in extracellular matrix protein modulation. *Cardiovasc. Res.* **87,** 628–635
65. Kasabova, M., Joulin-Giet, A., Lecaille, F., Saidi, A., Marchand-Adam, S., and Lalmanach, G. (2013) Human cystatin C: a new biomarker of idiopathic pulmonary fibrosis. *Proteomics Clin. Appl.*, 10.1002/prca.201300047